Electronic Supplementary Material (ESI) for Nanoscale.

Supporting Information

Oxidation behavior in layered Fe_nGeTe_2 (n = 3, 4, 5) and $Cr_2Ge_2Te_6$ governed by interlayer coupling

Yu Guo, Yanyan Zhao, Si Zhou*, Jijun Zhao*

Key Laboratory of Materials Modification by Laser, Ion and Electron Beams (Dalian University of Technology), Ministry of Education, Dalian 116024, China

*Corresponding authors. Email: sizhou@dlut.edu.cn; zhaojj@dlut.edu.cn

S1. Several atomic configurations for O_2 adsorption on Fe_nGeTe_2 and $Cr_2Ge_2Te_6$

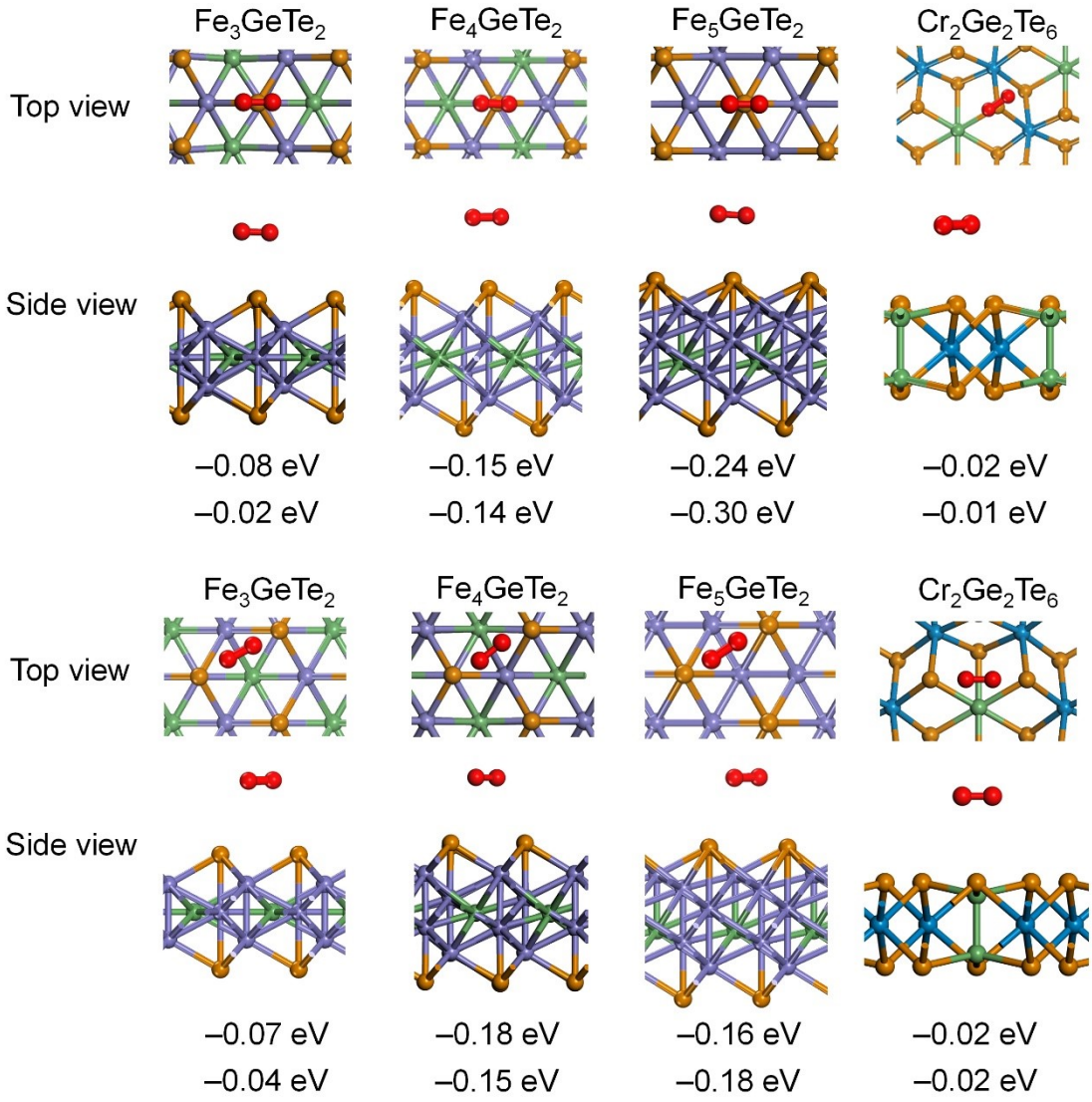

Fig. S1. Top and side views of local geometries for other O_2 adsorption sites for layered Fe_nGeTe_2 and $Cr_2Ge_2Te_6$. The numbers at the bottom indicate the binding energy of O_2 adsorption on the monolayer and bilayer surface, respectively.

S2. Bader charge analysis of Te atoms in the monolayer and bilayer systems

Table. S1. Bader charge (*e*) of Te atoms in the monolayer and bilayer systems. "Te-1st" and "Te-2nd" represent the Te atom at the surface and interlayer for the bilayers.

Bader Charge		Fe_3GeTe_2	Fe_4GeTe_2	Fe_5GeTe_2	$Cr_2Ge_2Te_6$
Monolayer	Te	6.25	6.12	6.14	6.35
Bilayer	Te-1st	6.23	6.10	6.07	6.35
	Te-2nd	6.27	6.14	6.15	6.35

S3. Another reaction pathway of O_2 adsorption on monolayer Fe_4GeTe_2

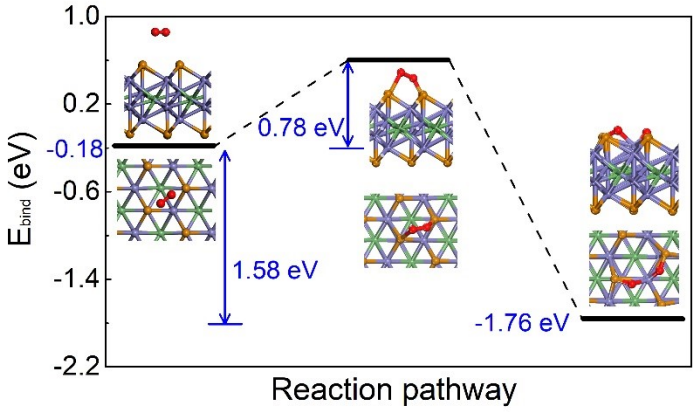

Fig. S2. Reaction pathway for a physisorbed O_2 molecule to dissociate and chemisorb on the surface of monolayer Fe_4GeTe_2. The black line segments indicate the energy levels of the initial state, transition state, and final state, respectively, with each corresponding atomic structures (top and side views) next to the energy level. The blue numbers give (from left to right) the binding energy of initial state, heat of reaction, activation energy, and binding energy of final state, respectively. Fe, Ge, Te and O atoms are shown in purple, green, orange and red, respectively.

S4. Oxidation behavior of Fe_nGeTe_2 at bulk limit

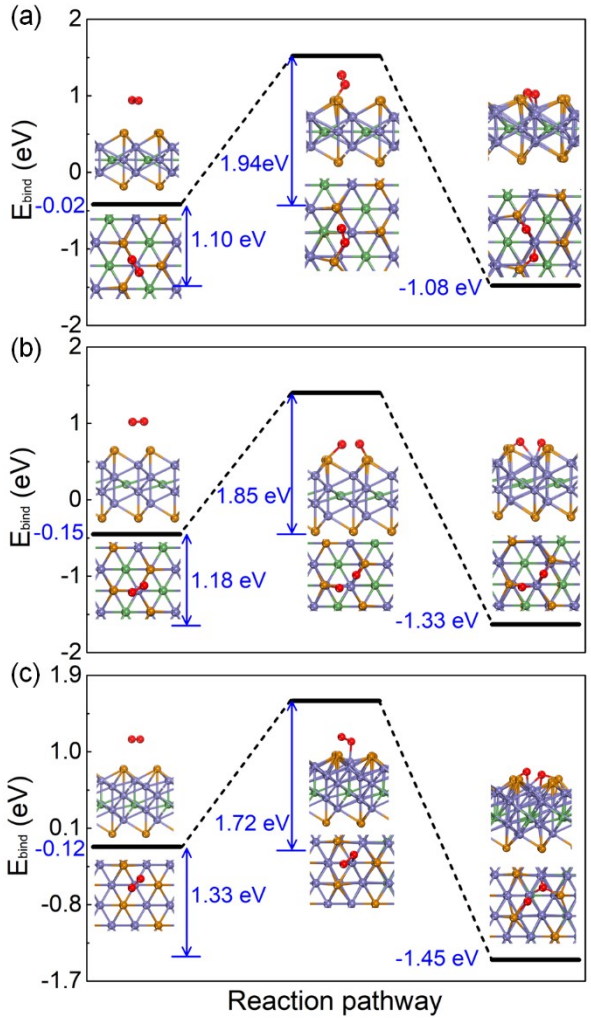

Fig. S3. Reaction pathway for a physisorbed O_2 molecule to dissociate and chemisorb on the surface of quadrilayer (a) Fe_3GeTe_2, (b) Fe_4GeTe_2 and (c) Fe_5GeTe_2, respectively. The black line segments indicate the energy levels of the initial state, transition state, and final state, respectively, with each corresponding atomic structures (top and side views) next to the energy level. The blue numbers (from left to right) give the binding energy of initial state, heat of reaction, activation energy, and binding energy of final state, respectively. Fe, Ge, Te and O atoms are shown in purple, green, orange and red, respectively.

S5. Reaction pathway of O_2 adsorption on layered Fe_nGeTe_2 and $Cr_2Ge_2Te_6$ using DFT+U method

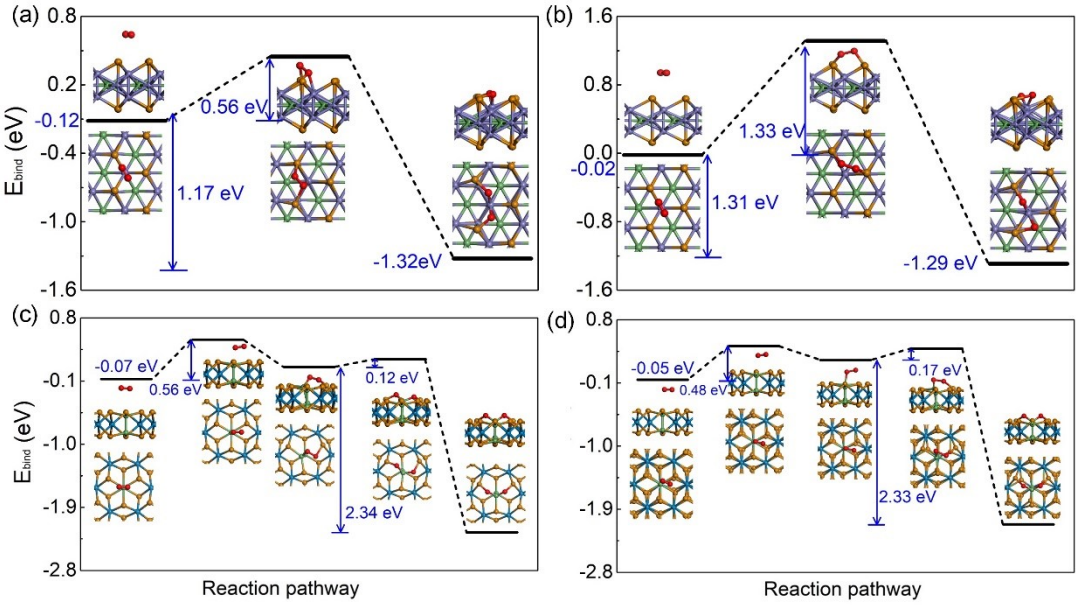

Fig. S4. Reaction pathway for a physisorbed O_2 molecule to dissociate and chemisorb on the surface of monolayer (left panels) and bilayer (right panels) for (a-b) Fe_3GeTe_2, and (c-d) $Cr_2Ge_2Te_6$, respectively, by using DFT+U method. Fe, Cr, Ge, Te and O atoms are shown in purple, blue, green, orange and red, respectively.

S6. AIMD simulations of O_2 reaction with monolayer and bilayer Fe_3GeTe_2 at 300 K

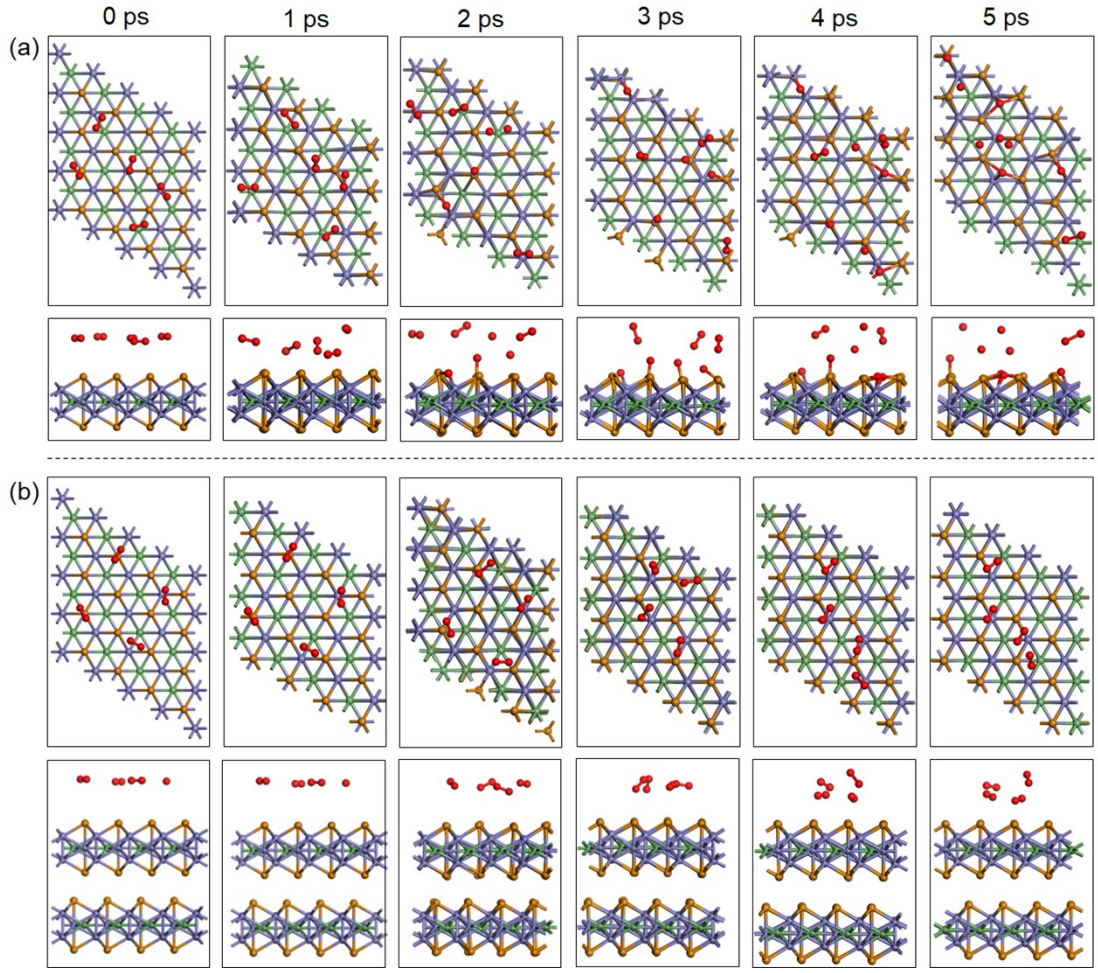

Fig. S5. Snapshots of AIMD simulations of O_2 oxidation for (a) monolayer and (b) bilayer Fe_3GeTe_2 at 300 K at 0 ~ 5 ps.

S7. Interlayer differential charge density of bilayer systems

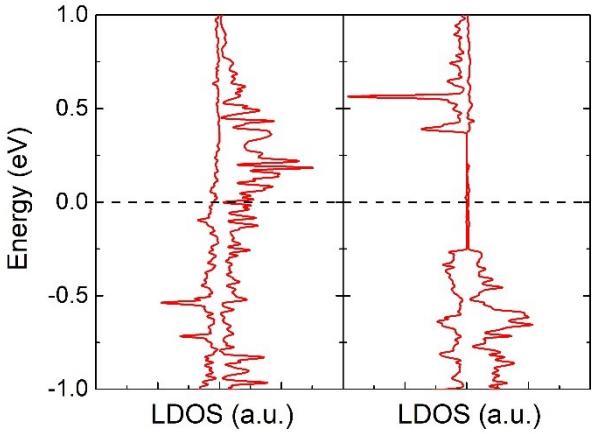

Fig. S6. LDOS of O atoms for monolayer and bilayer Fe_5GeTe_2 at oxidation transition states from left to right panels, respectively.

S8. Wavefunction norm of monolayer and bilayer Fe_nGeTe_2 during oxidation process

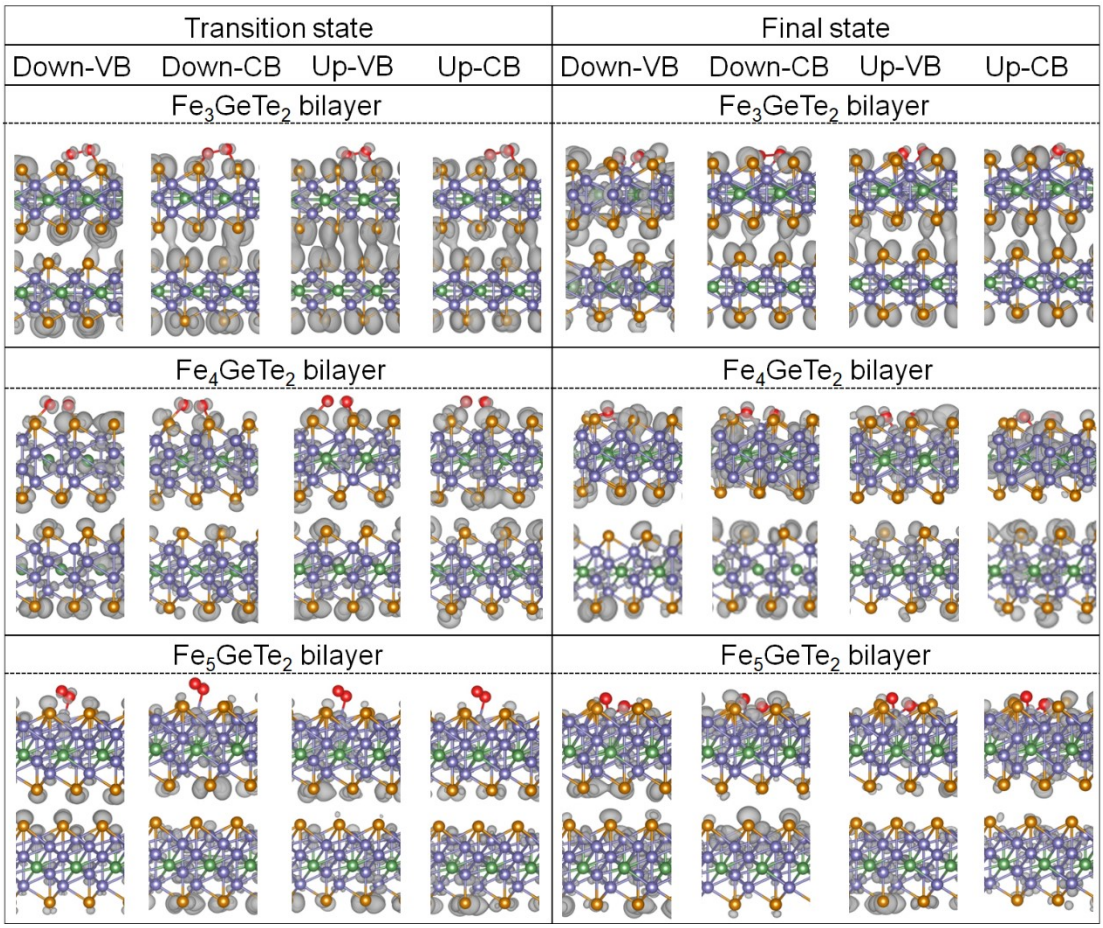

Fig. S7. Side view of the wavefunction norm of spin-up and spin-down VBM and CBM at Γ point with an isosurface value of 1×10^{-5} $|e|/Å^3$ for the transition and final states of bilayer Fe_nGeTe_2 during oxidation process. Fe, Ge and Te atoms are shown in purple, green and orange, respectively.

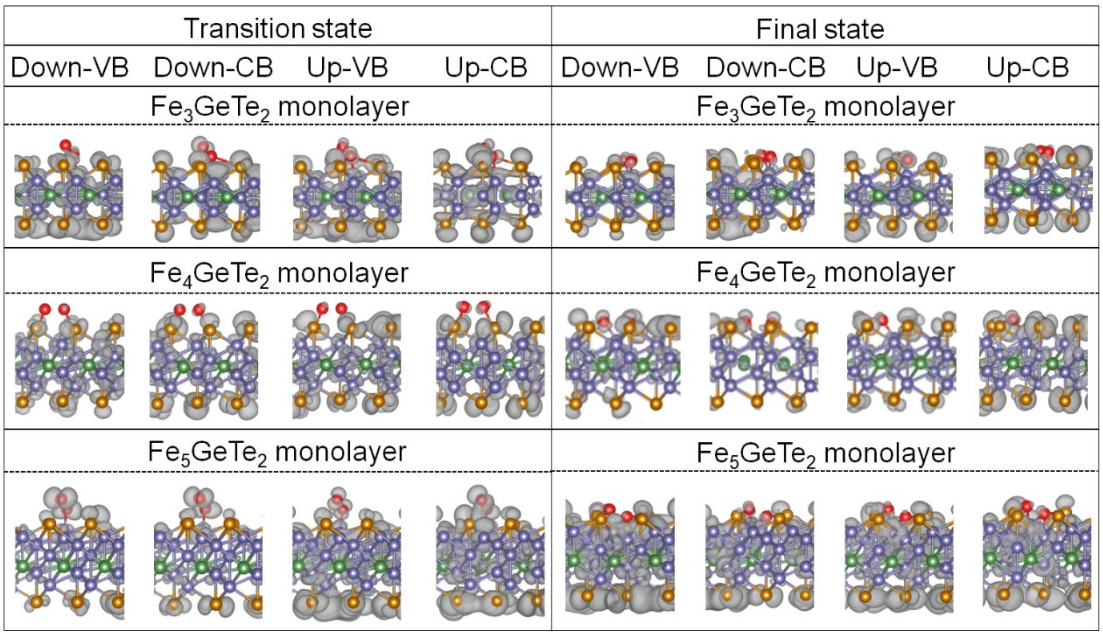

Fig. S8. Side view of the wavefunction norm of spin-up and spin-down VBM and CBM at Γ point with an isosurface value of 1×10^{-5} $|e|/Å^3$ for the transition and final states of monolayer Fe_nGeTe_2 during oxidation process. Fe, Ge and Te atoms are shown in purple, green and orange, respectively.

S9. O−O bond length during Fe_nGeTe_2 oxidation process

Table S2. O−O bond length (Å) for the oxidized Fe_nGeTe_2

O-O bond length		Initial	Transition	Final
Fe_3GeTe_2	Monolayer	1.23	1.37	2.43
	Bilayer	1.23	1.37	2.59
Fe_4GeTe_2	Monolayer	1.23	1.9	2.56
	Bilayer	1.23	1.79	2.43
Fe_5GeTe_2	Monolayer	1.25	1.31	2.53
	Bilayer	1.25	1.32	2.52

S10. Charge transfer between O atom and Fe_nGeTe_2 surface

Table S3. Charge transfer between O atom and Fe_nGeTe_2 surface at final oxidation state

Charge transfer (e)		
Fe_3GeTe_2	Monolayer	1.91
	Bilayer	1.89
Fe_4GeTe_2	Monolayer	2.42
	Bilayer	2.25
Fe_5GeTe_2	Monolayer	1.84
	Bilayer	1.80

S11. Wavefunction norm of monolayer and bilayer Fe_nGeTe_2 and $Cr_2Ge_2Te_6$ with DFT+U method

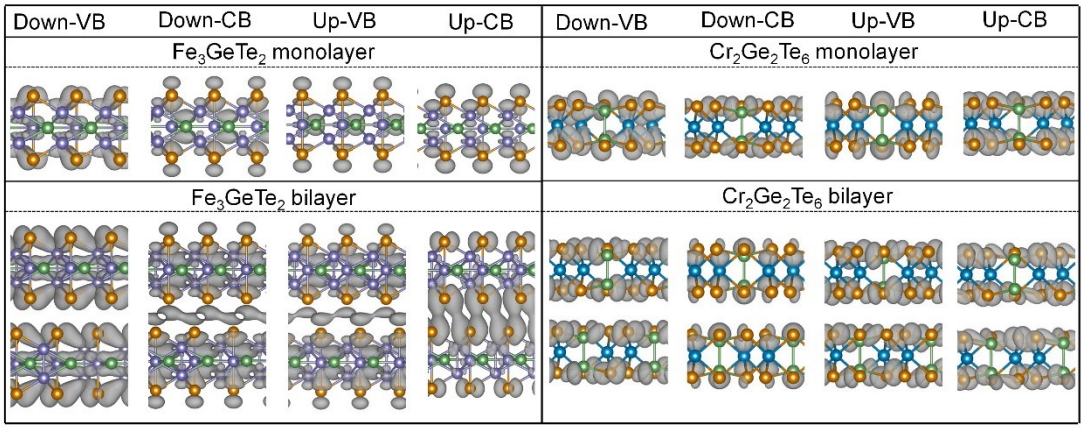

Fig. S9. Side view of the wavefunction norm of spin-up and spin-down VBM and CBM at Γ point with an isosurface value of 1×10^{-5} $|e|/Å^3$ for monolayer and bilayer Fe_3GeTe_2 and $Cr_2Ge_2Te_6$ by using DFT+U method. Fe, Cr, Ge and Te atoms are shown in purple, blue, green and orange, respectively.

S12. Interlayer differential charge density of bilayer systems

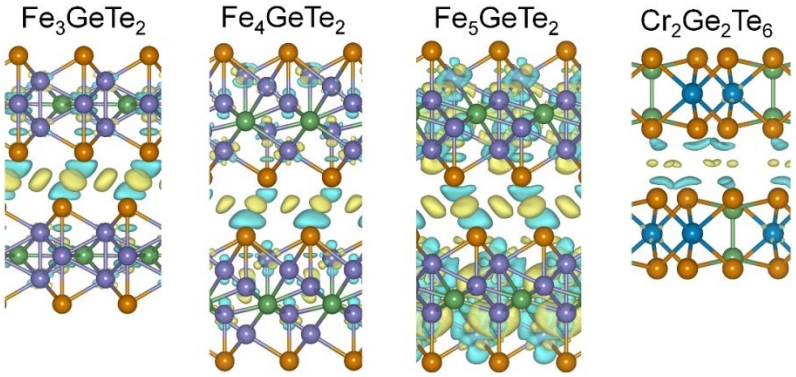

Fig. S10. Interlayer differential charge density of bilayer Fe_3GeTe_2, Fe_4GeTe_2, Fe_5GeTe_2 and $Cr_2Ge_2Te_6$ from side view. Fe, Cr, Ge and Te atoms are shown in purple, blue, green and orange, respectively. The cyan and yellow indicate the electron depletion and accumulation regions, respectively, with isosurface value of 0.0003 $|e|/Å^3$.

S13. Several different antiferromagnetic configurations of monolayer systems

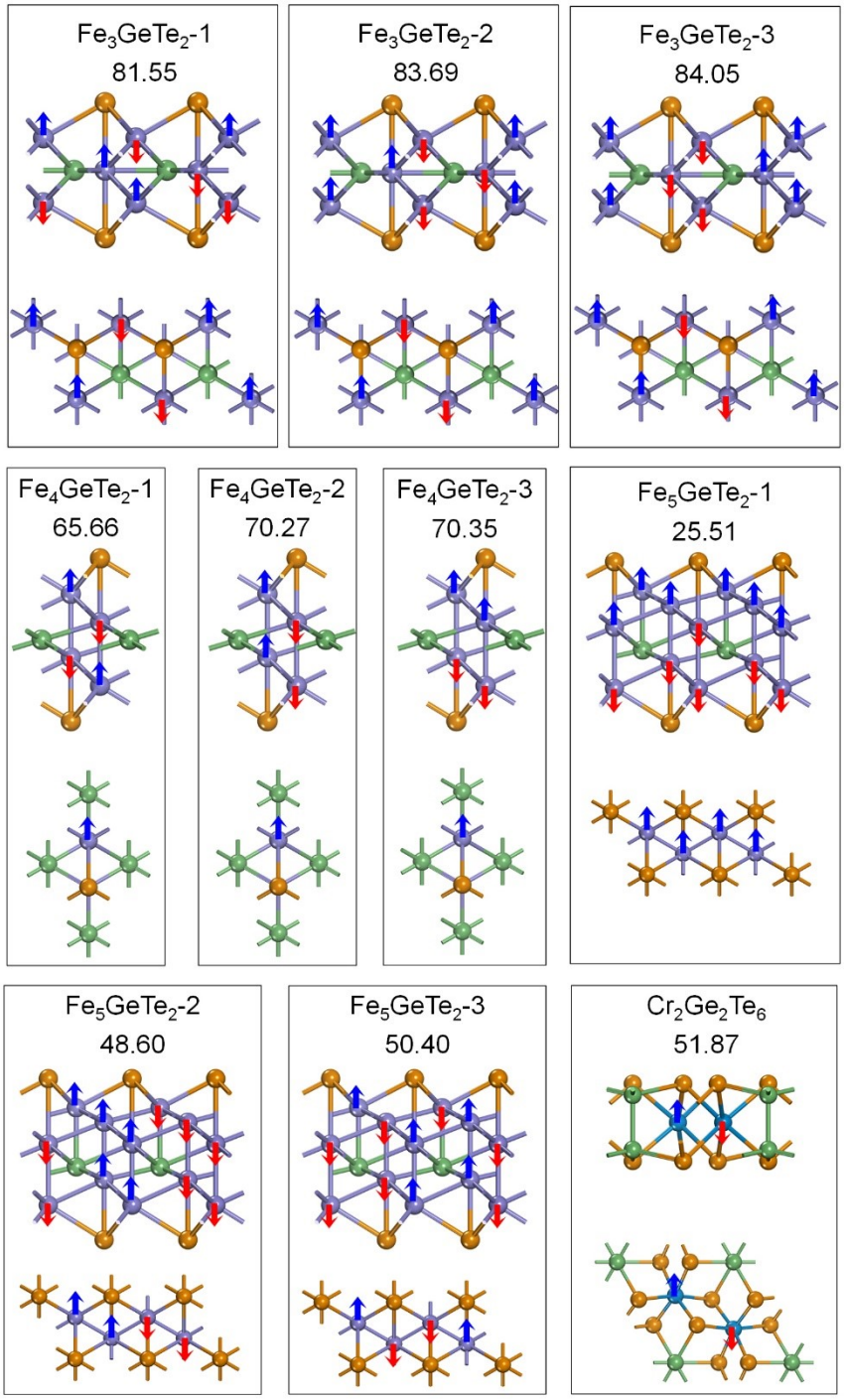

Fig. S11. Several different antiferromagnetic configurations for monolayer Fe_3GeTe_2, Fe_4GeTe_2, Fe_5GeTe_2 and $Cr_2Ge_2Te_6$ from side and top views. The black numbers at the top of each panel represent exchange energy (ΔE in the unit of meV/Fe or Cr atom). Fe, Cr, Ge and Te atoms are shown in purple, blue, green and orange, respectively.

S14. The interlayer distance of bilayer Fe_nGeTe_2 and $Cr_2Ge_2Te_6$ after oxidation

Table S4. The interlayer distance (Å) of bilayer Fe_nGeTe_2 and $Cr_2Ge_2Te_6$ after oxidation at initial and final states.

	Pristine	Initial	Final
Fe_3GeTe_2	2.94	2.90	2.93
Fe_4GeTe_2	3.04	3.02	2.97
Fe_5GeTe_2	3.14	3.13	3.12
$Cr_2Ge_2Te_6$	3.42	3.41	3.39